J Appl Electrochem (2011) 41:687–694
DOI 10.1007/s10800-011-0281-4

ORIGINAL PAPER

Electrochemical simultaneous determination of nitrophenol isomers at nano-gold modified glassy carbon electrode

Lin Chu · Lu Han · Xiaoli Zhang

Received: 14 December 2010 / Accepted: 3 March 2011 / Published online: 15 March 2011

Abstract A novel method for simultaneous determination of nitrophenol isomers at nano-gold modified glassy carbon electrode has been developed. The gold nanoparticles were directly electrodeposited onto the glassy carbon electrode via a constant potential −0.2 V (vs. SCE) for 60 s from 0.1 mol L^{-1} KNO_3 containing 0.4 g L^{-1} $HAuCl_4$. The resulting electrode (nano-Au/GCE) was characterized with scanning electron microscopy (SEM). The electrochemistry response of nitrophenol isomers at the nano-Au/GCE was studied. The result indicated that *o*-, *m*-, and *p*- nitrophenol are separated entirely at nano-Au/GCE, and a semi-derivative voltammetric technology was adopted to enhance the determination sensitivity. This modified electrode could be applied to direct simultaneous voltammetric determination of nitrophenol isomers in water samples without preseparation with higher sensitivity.

Keywords Nano-gold-modified electrode · Simultaneous determination · Nitrophenol isomers · Voltammetry

1 Introduction

Phenol and substituted phenols are among the most toxic substances and are widely distributed in industrial and natural waste. Nitrophenols are considered by the United States Environmental Protection Agency (USEPA) as priority pollutants due to the fact that they have serious effects on human beings, animals, and plants [1]. Because of nitrophenols' detriment and vast scale distributions in the ecological environment, the detection of them has become one of the important studies of environmental analysis. At present, the main analytical methods for nitrophenols are chromatography and spectrophotometry [2–5]. Nitrophenols have three isomers. The simultaneous determination of isomers at the conventional electrode by voltammetry is difficult owing to their reductive or anodic peak potentials close to each other. Ni et al. reported a simultaneous determination of nitro-substituted phenols by differential pulse voltammetry at a hanging mercury drop electrode, and chemometrics methods of data analysis were applied to resolve the overlapped reductive peaks [6]. In recent years, various chemically modified electrodes (CMEs) were used for nitrophenol isomers determination, the resolution of isomers was improved based on the different kinds of the modifier [7–9].

Recently, gold nanoparticles as a kind of special sensing material of chemical modified electrodes show excellent electrical conductivity, electrocatalytic activity, and chemical stability. Gold nanoparticles provide a new avenue for fabricating electrochemical devices because it can facilitate electron transfer between electroactive species and electrodes. Gold nanoparticle-modified electrodes were generally obtained with assembling nanoparticles onto the basement electrode by variety of chemical techniques, such as electrodeposition from the colloids [10–12], Langmuir–Blodgett (LB) technique [13, 14], and layer-by-layer (LBL) assembly method [15–17]. In contrast, the direct electrodeposition from $AuCl_4^-$ solution to obtain gold nanoparticle-modified electrode is a rapid and easy alternative method for the preparation of modified electrode in a short time. Very recently, we reported the electrodeposition preparation of nanogold modified GCE and its application for voltammetric determination of dihydroxybenzene isomers [18].

L. Chu · L. Han · X. Zhang (✉)
School of Chemistry and Chemical Engineering,
Shandong University, Jinan 250100, China
e-mail: zhangxl@sdu.edu.cn

In this article, we proposed the simultaneous determination of nitrophenol isomers by voltammetry at the nano-gold modified glassy carbon electrode. Compared with the carbon nanotube modified glassy carbon electrode by Luo [19], the proposed method to prepare the modified electrode is more convenient and controllable. The *o*-, *m*-, and *p*- nitrophenol were separated entirely at the nano-gold modified glassy carbon electrode with wide linear range and high selectivity.

2 Experimental

2.1 Apparatus and reagents

A CHI 800 electrochemical analyzer (Shanghai Chenhua Instrument Company, China) was used to perform electrode characterization and voltammetric measurements. A conventional three-electrode system, including a bare glassy carbon electrode (4 mm diameter) or a Au electrode (4 mm diameter) or modified glassy carbon electrode as working electrode, a saturated calomel electrode (SCE) as reference electrode and a platinum plate as counter electrode was used in this study. All potentials in the text were against SCE. Deaeration was performed by purging with nitrogen gas.

o-, *m*-, *p*-nitrophenol and $HAuCl_4$ (obtained from Shanghai Chemical Reagents Co. Ltd) were used without further purification, and their stock solutions were stored at −4 °C away from light. All the chemicals used were analytical reagent grade. Doubly distilled water was used to prepare the solution.

2.2 Preparation of the nano-gold modified electrode

The GCE surface was polished to a mirror-like surface with alumina slurries, and then washed with absolute ethanol and water in an ultrasonic bath for 5 min. Finally, the clean electrode was immersed into 0.1 mol L^{-1} KNO_3 containing 0.4 g L^{-1} $HAuCl_4$ and electrodeposition from $HAuCl_4$ was conducted at −0.2 V (vs.SCE) for 60 s. Then the resulting electrode (nano-Au/GCE) was taken out and rinsed with water.

2.3 Analytical procedure

Unless other stated, 0.1 mol L^{-1} buffer solution Na_2HPO_4–NaH_2PO_4 (pH 6.0) was used as the supporting electrolyte for determination of nitrophenol isomers. Firstly, the solution was degassed with N_2 and kept under N_2 blanket. Then, the voltammograms of nitrophenol isomers were recorded from −0.6 to 0.6 V. Finally, the voltammetric curves were treated using a semi-derivative technique on the CHI-800 electrochemical workstation.

3 Results and discussion

3.1 Morphology of as-prepared gold nano-structured layer

Nano-gold modified electrode was fabricated by electrodepositing gold onto the polished GCE in 0.1 mol L^{-1} KNO_3 solution containing $HAuCl_4$. The size and morphology of deposited gold particles could be controlled to some extent through choosing deposition time and the concentration of $HAuCl_4$. Figure 1 shows the morphology of as-prepared nano-gold structured layer under different deposition time characterized by scanning electron microscopy (SEM). The conditions for Fig. 1 are a 0.4 g L^{-1} $HAuCl_4$ solution, −0.2 V (vs.SCE) depositing potential. The deposition time is 20, 180, and 350 s, respectively. In Fig. 1b, clear small deposits can be seen, while there are no such features seen on clean GCE surface which is smooth (Fig. 1a). It shows that visible gold nanoparticles are first generated within just 20 s of deposition. Besides, it can be seen that the increasing in the deposition time results in the augmentation of the average particle size of nano-gold particles (Fig. 1b–d). The average diameter of the particles is about 20 nm (Fig. 1b) and 50 nm (Fig. 1c), respectively. For growth from 0.4 g L^{-1} $HAuCl_4$, increasing the deposition time up to or beyond 180 s causes the agglomeration of nanoparticles. The longer deposition time (up to or beyond 350 s) causes the formation of a staggered multi-layer structure (Fig. 1d).

3.2 Voltammetric behavior of nitrophenol isomers at nano-Au/GCE

To examine the electrocatalytic performance of nano-Au/GCE, cyclic voltammetry was employed first. Figure 2 shows the typical cyclic voltamograms of *o*-, *m*-, and *p*-nitrophenol mixture in the potential range from −0.6 to +0.6 V (vs.SCE) at bare GCE, bare Au and nano-Au/GCE electrode. It can be seen that at the bare GCE (dash line), *o*-nitrophenol gives a very weak oxidation peak at 0.240 V. Although *o*-nitrophenol can be separated from *m*- and *p*-nitrophenol, the voltammogram of *m*- and *p*-nitrophenol overlaps to form a wide oxidation peak at about 0.06 V. Moreover, at cathodic branch, three isomers also have no obvious reduction peaks. The phenomenon at bare Au electrode is similar to bare GCE (dot line). Namely nitrophenol isomers could not be discriminated at bare GCE or bare Au electrode. However, at the nano-Au/GCE (solid line), three well-defined oxidation peaks (a_2, a_3, and a_4) appear at 0.016, 0.158, and 0.250 V corresponding to *m*-, *p*-, and *o*-nitrophenol, respectively. The oxidation peak potential difference between *o*- and *p*-nitrophenol is 92 mV, *p*- and *m*-nitrophenol is 142 mV. Meanwhile, compared

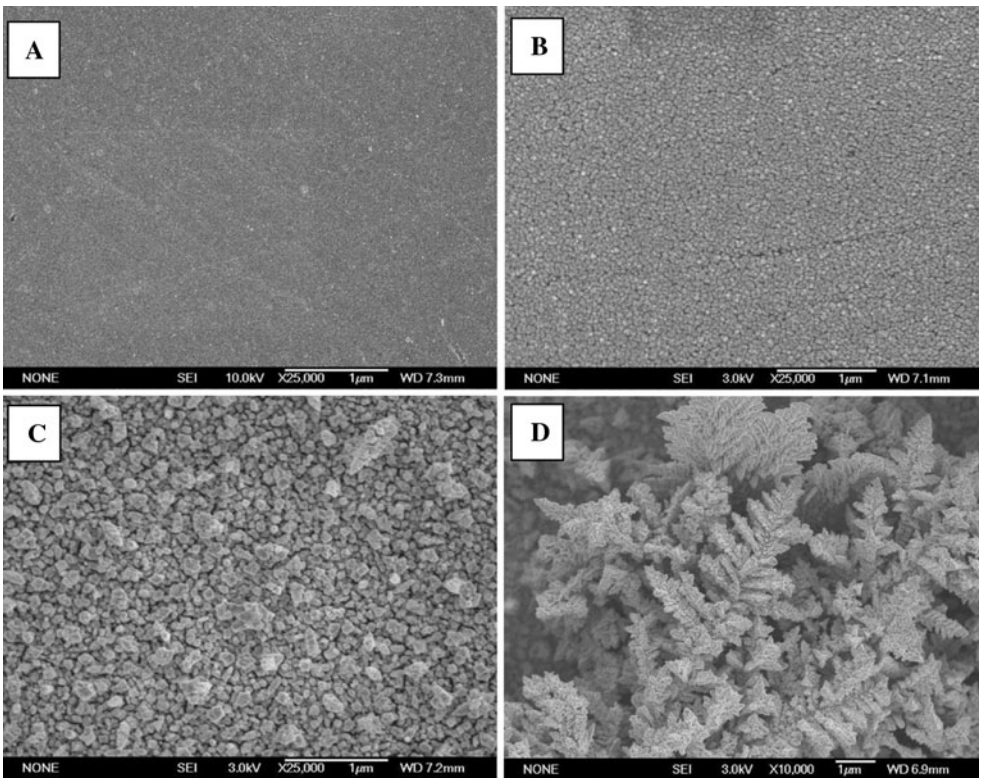

Fig. 1 SEM images of **a** bare GCE and **b–d** nano-Au/GCE prepared via different electrodeposition time. **b** 20 s, **c** 180 s, **d** 350 s. The deposition potential was −0.2 V (vs.SCE). The concentration of $HAuCl_4$ was 0.4 g/L

with both bare GCE and bare Au electrode, the peak currents increase significantly. The results indicate that the nano-Au/GCE not only identify simultaneously the nitrophenol isomers, but also greatly enhance the detection sensitivity. The reason may be that the nano-Au/GCE has a large surface area and a great deal of active sites, better conductivity and favorable electrocatalytic power, all of them contribute to the dissimilar conformation of *o*-, *m*-, and *p*-nitrophenol. Therefore, nitrophenol isomers show different electrochemical potentials and free-energy at this electrode surface. In addition, at cathodic sweep branch, three well-separated reduction peaks (c_2, c_3, and c_4) can also be observed. The peak potential is 0.202, 0.097, and −0.028 V, corresponding to *o*-, *p*-, and *m*-nitrophenol, respectively, which could also be used for simultaneous determination of nitrophenol isomers (The oxidation peak is chosen as research objects in this article). Besides, there is still a reduction peak (c_1) at about −0.450 V. This peak c_1 is reduction of the nitryl in nitrophenol. On the voltammograms, three isomers only gave a nitryl reduction peak meaning the existence of coincidence peak. Therefore, it is not used for isomers determination based on the nitryl reduction at nano-Au/GCE. When a semi-derivative technology is used to treat the voltammetric curve, the more available peak height can be obtained (Fig. 2, inset, solid line).

In addition, we contrasted the voltammetric response *o*-, *m*-, and *p*-nitrophenol at nano-Au/GCE with that at nano-Au/Au under the same conditions. The result suggests that the peak potential and peak height of the three isomers are nearly same (Figure was not shown). In this article, the glassy carbon electrode was chosen as the basement electrode.

In order to conclude the electrochemical reaction mechanism for the nitrophenol isomers at nano-Au/GCE, the continuous cyclic voltammograms are recorded (shown in Fig. 3a). The voltammograms of *o*-, *m*-, and *p*-nitrophenol are started from positive to negative (from 0.6 to −0.8 V, it is different from Fig. 2 at direction of the scanning voltage, which results in small differences in peak potential of *o*-, *m*-, and *p*-nitrophenol compared with that in Fig. 2). During the first cycle, one reduction peak (c_1) appears in the cathodic sweep branch, three oxidation peaks (a_2, a_3, and a_4) appear in the anodic sweep branch (solid line). However, in the second cycle, in addition to peak c_1, three new reduction peaks (c_2, c_3, and c_4) also appear in the cathodic sweep branch (dash line).

To further make clear the reaction pathway, the different scan potential ranges are examined. Figure 3b shows the

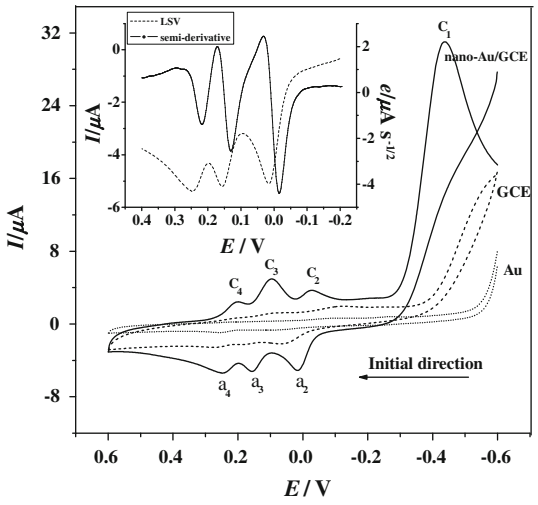

Fig. 2 Cyclic voltammograms and semi-derivative voltammograms (*inset*) of *o*-, *m*-, and *p*- nitrophenol mixture (1×10^{-4} mol L^{-1} for each) in the 0.1 mol L^{-1} Na_2HPO_4–NaH_2PO_4 (pH 6.0) solution at GCE (*dash line*), Au (*dot line*) and nano-Au/GCE (*solid line*). The conditions of prepared nano-Au/GCE electrode were 0.4 g L^{-1} $HAuCl_4$, −0.2 V (vs.SCE) deposition potential and 60 s deposition time. The radius of GCE and Au was 2 mm, and the radius of basement GCE for nano-Au/GCE was also 2 mm. Potential scan rate was 100 mV s^{-1}

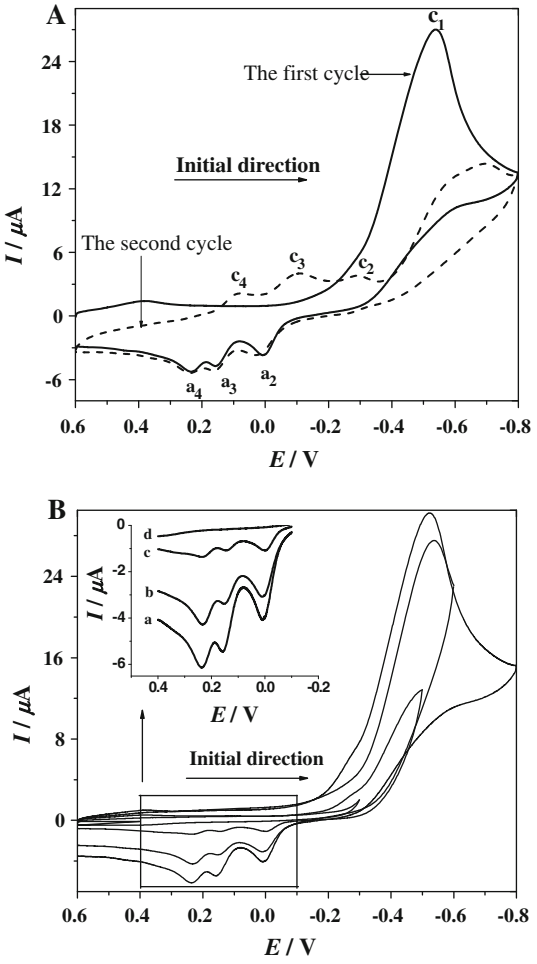

Fig. 3 **a** The continuous cyclic voltammograms of *o*-, *m*-, *p*-nitrophenol mixture (1×10^{-4} mol L^{-1} for each) at nano-Au/GCE. **b** First cycle voltammograms of *o*-, *m*-, *p*-nitrophenol mixture in the different scan potential ranges. (*a*) 0.6 to −0.8 V, (*b*) 0.6 to −0.6 V, (*c*) 0.6 to −0.5 V, (*d*) 0.6 to −0.3 V

voltammograms of *o*-, *m*-, and *p*-nitrophenol in the different scan potential ranges (from 0.6 to −0.8, 0.6 to −0.6, 0.6 to −0.5, and 0.6 to −0.3 V, respectively, for curve *a*–*d*). It can be seen that the peak couples, a_2/c_2, a_3/c_3, and a_4/c_4, disappear gradually with scan retrace potential changing from −0.8 to −0.3 V (Fig. 3b, inset). These phenomena indicate that the appearance of peak couples, a_2/c_2, a_3/c_3, and a_4/c_4, are concerned with the nitryl reduction of peak c_1, meaning that the products of nitrophenol by irreversible reduction remain on or close to the modified electrode surface and are oxidized again on the subsequent anodic scan. This conclusion is consistent with that reported by Luo [19]. Moreover, Hu [7], Mhammedi [20], Compton [21], and Kubota [22] also reported that *p*-nitrophenol could be transferred to *p*-hydroxylaminophenol (ϕNHOH) via the irreversible four-electron transfer, while *p*-hydroxylaminophenol could be transferred easily to *p*-nitrosophenol (ϕNO) by the reversible two-electron oxidation/reduction. Therefore, we may conclude with considerable assurance that the same electron transfer mechanism can be applied at nano-Au/GCE electrode in our studies:

$$\phi NO_2 + 4H^+ + 4e^- \rightarrow \phi NHOH + H_2O \ (c_1)$$
$$\phi NHOH - 2H^+ - 2e^- \rightarrow \phi NO \ (a_2/c_2 a_3/c_3 a_4/c_4)$$

However, the formed peak sequences in our works are different from the literature [19]. On the voltammetric curve, from negative to positive, the arrangements of redox couples are *m*-, *p*-, and *o*-nitrophenol (see Fig. 2). Scilicet, the reduction product of *m*-nitrophenol, *m*-hydroxylaminophenol, was much more easily oxidation, and its oxidation peak potential was the most negative. And the reduction product of *o*-nitrophenol, *o*-hydroxylaminophenol, was the most difficult which resulting in the most positive oxidation peak potential. The explanation for this arrangement may be owing to different molecule structures of *m*-, *p*-, and *o*-hydroxylaminophenol and disparate constellation or overlap with electrode surface. As all known that substituting group in the benzene ring can influence the density of electron cloud through conjugation effect (C effect) and inductive effect (I effect). The C effect plays a more important role than I effect does. Therefore, the electron cloud was shared greatly in *o*- or *p*-hydroxylaminophenol. Meanwhile, the conjugation extent between the *o*- or *p*-hydroxylaminophenol and electrode surface was

larger than that in *m*-hydroxylaminophenol, which results in their lower free-energy. Thus, the oxidation peak potential of *o*- or *p*-hydroxylaminophenol was more positive than that of *m*-hydroxylaminophenol. With regard to *o*- or *p*-hydroxylaminophenol, when hydroxylamino group occupies *o*-position, a chelate molecule was formed through intermolecular hydrogen bonds between the hydrogen and the oxygen, which led to a larger steric hindrance than *p*- during reaction. Thus, the electrochemical oxidation of hydroxylaminophenol became more and more difficult from *m*- to *p*- to *o*-, and the potentials of oxidation peak shifted positively.

3.3 Influence of deposition time

The response of nitrophenol isomers at nano-Au/GCE electrode was strongly deposition time dependent. The prepared nano-Au/GCE based on different deposition times (20, 60, 120, 180, and 350 s) was examined to detect *o*-, *m*-, and *p*-nitrophenol using linear sweep voltammetry (shown in Fig. 4a). As the deposition time increased from 20 to 180 s, the peak current increased gradually due to gold nanoparticles increment and surface area multiplication.

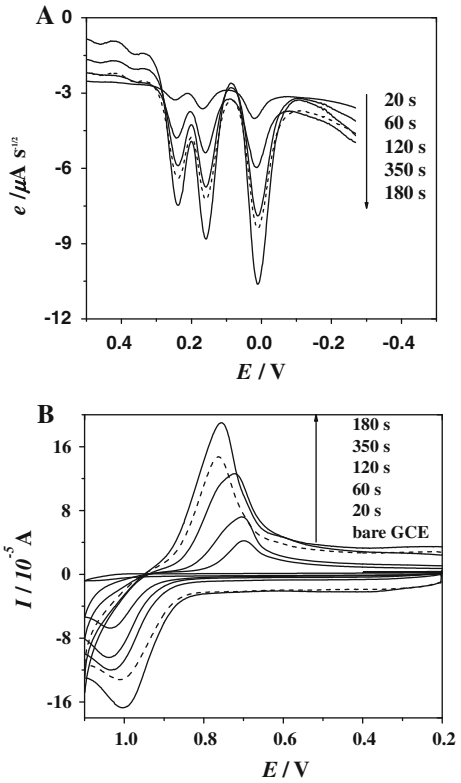

Fig. 4 **a** The semi-derivative voltammetric curves of *o*-, *m*-, *p*-nitrophenol mixture (1×10^{-4} mol L^{-1} for each) at nano-Au/GCE prepared with different deposition time (20, 60, 120, 180, 350 s). **b** Cyclic voltammograms of 1 mmol L^{-1} $Ru(bpy)_3^{2+}$ in 0.2 mol L^{-1} Na_2SO_4 at GCE and nano-Au/GCE prepared with different deposition time (20, 60, 120, 180, 350 s). The scan rate was 50 mV s^{-1}

When the deposition time exceeded 350 s, the peak current decreased greatly (Fig. 4a, dash line). The reason may be that the agglomeration of nanoparticles results in the electrode surface area decrease. To confirm the fact of area change, a cyclic voltammetric study for the nano-Au/GCE prepared via different deposition times was performed utilizing a redox probe, $Ru(bpy)_3^{2+}$. It was expected that the electron transfer reaction and peak current would be enhanced with electrode surface area multiplication. Figure 4b supports this expectation. The responses of 1 mmol L^{-1} $Ru(bpy)_3^{2+}$ in 0.2 mol L^{-1} Na_2SO_4 at nano-Au/GCE are increased with the deposition time from 20 to 180 s. When the deposition time up to or beyond 350 s, the peak current decreased compared with that at 180 s (Fig. 4b, dash line).

The above results indicate that the control of the particle size along with its size distribution plays a very important role in the determination of nitrophenol isomers.

3.4 Influence of pH

In order to optimize the responses of *o*-, *m*-, and *p*-nitrophenol at nano-Au/GCE, a series of supporting electrolytes were tested, such as tris–HCl, $Na_2B_4O_7{\cdot}10H_2O$, $C_8H_8O_7{\cdot}H_2O$, KNO_3, and Na_2HPO_4–NaH_2PO_4. The results demonstrated that the *o*-, *m*-, and *p*-nitrophenol gave the most sensitive oxidation peak using Na_2HPO_4–NaH_2PO_4 as supporting electrolyte. In addition, five different concentrations of Na_2HPO_4–NaH_2PO_4 solution (0.01, 0.05, 0.1, 0.5, and 1 mol L^{-1}) were tested, the result was that the peak height for three isomers almost keep unalterable. Considering both of the buffer capacity and interference, 0.1 mol L^{-1} concentration of Na_2HPO_4–NaH_2PO_4 buffer was selected for further experiments. Figure 5 shows the influence of electrolyte pH level on peak current and peak separation of the three isomers. As can be seen from Fig. 5a, the peak height rises with the increase of pH in the range of 3.0–5.0 and gives a maximum at pH 5.54. At the pH value exceeds 7.0, the peak height decreases fleetly and nearly no peak is observed at pH 8.0. The reason might be that the electro-redox of nitrophenol isomers is a proton-participating reaction just as what the reaction mechanism concluded. Thus, acidity of solution would affect the electro-redox behavior of nitrophenol isomers. In low pH values, the nitryl reduction would be interfered by H^+ response, while at high pH values (pH exceeds 8.0), the *o*-, *m*-, *p*-nitrophenol (p*K*a = 7.21, 8.0, 7.15, respectively) can be ionized and negatively charged, which results in a mutual repulsion between the nitrophenol and negatively charged modified film on the electrode surface. As a result, the peak current decrease.

Figure 5b shows the relationship between the pH value and the oxidation peak potential. The results show that the peak potentials of the three isomers move collectively more

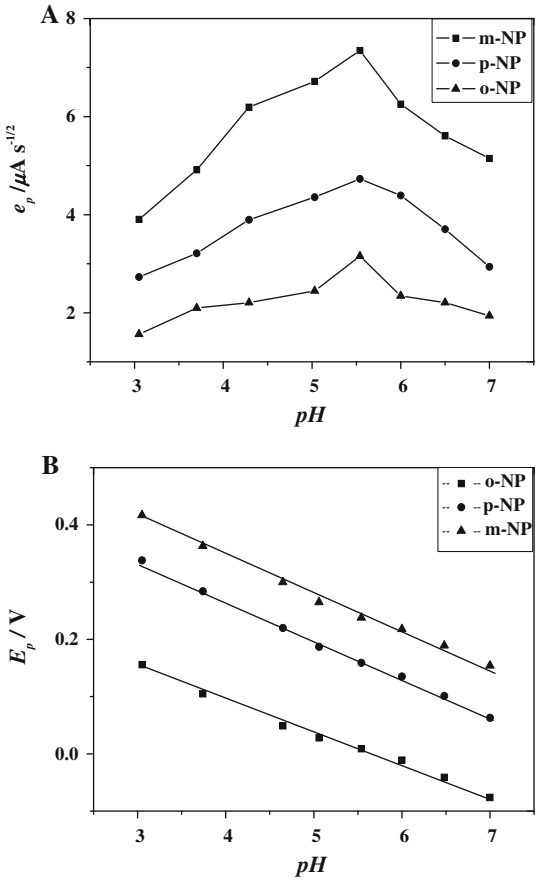

Fig. 5 **a** The influence of pH on the peak height of *o*-, *m*-, *p*-nitrophenol mixture (1×10^{-4} mol L^{-1} for each). **b** The influence of pH on the peak potentials of *o*-, *m*-, *p*-nitrophenol (1×10^{-4} mol L^{-1} for each)

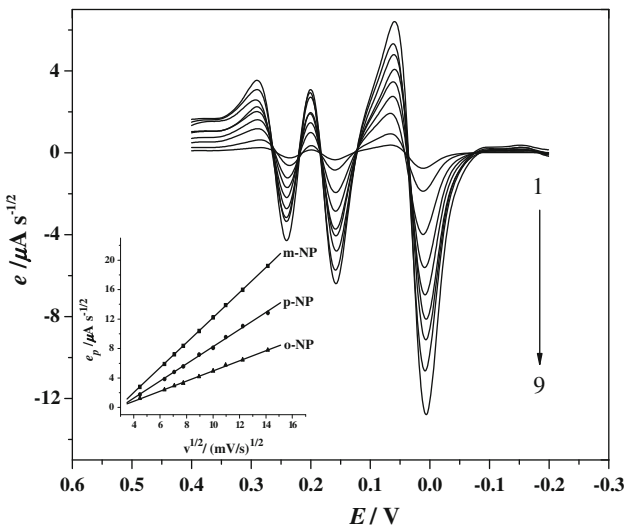

Fig. 6 The semi-derivative voltammetric curves of *o*-, *m*-, *p*-nitrophenol (1×10^{-4} mol L^{-1} for each) under different scan rate at nano-Au/GCE. Scan rates (1–9): 20, 40, 50, 60, 80, 100, 120,150, 200 mV s^{-1}. *Inset* The relation between the peak heights versus the square roots of scan rate

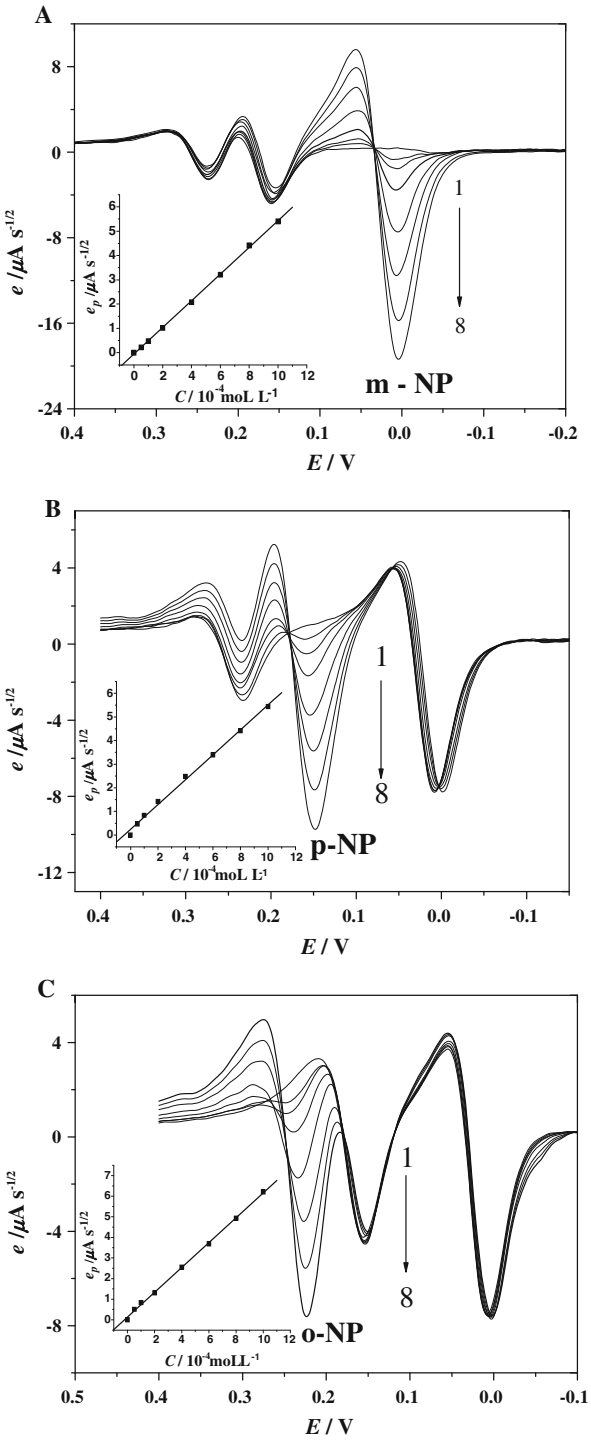

Fig. 7 The semi-derivative voltammetric responses of various concentrations of *o*-, *m*-, *p*-nitrophenol at nano-Au/GCE. **a** *o*-nitrophenol 4.0×10^{-4} mol L^{-1}, *m*-nitrophenol 4.0×10^{-4} mol L^{-1}, *p*-nitrophenol (1–8) 0, 0.5, 1.0, 2.0, 4.0, 6.0, 8.0, 10.0×10^{-4} mol L^{-1}; **b** *o*-nitrophenol 4.0×10^{-4} mol L^{-1}, *p*-nitrophenol 4.0×10^{-4} mol L^{-1}, *m*-nitrophenol (1–8) 0, 0.5, 1.0, 2.0, 4.0, 6.0, 8.0, 10.0×10^{-4} mol L^{-1}; **c** *p*-nitrophenol 4.0×10^{-4} mol L^{-1}, *m*-nitrophenol 4.0×10^{-4} mol L^{-1}, *o*-nitrophenol (1–8) 0, 0.5, 1.0, 2.0, 4.0, 6.0, 8.0, 10.0×10^{-4} mol L^{-1}. *Inset* The relation between the peak heights versus the different concentrations of *o*-, *m*-, *p*-nitrophenol

negative values with the raise of pH value. The peak potential, E_p, versus pH has a good linear relation in the range of pH 3.0–7.0 and the three lines are nearly parallel, meaning that the change of pH value has no influence on the resolution of nitrophenol isomers.

3.5 Effect of scan rate

The effect of scan rate on oxidation peak height at the nano-Au/GCE was displayed at Fig. 6. The peak height rises with the increase of scan rate. That exhibits a linear relation to the square root of the scan rate in the range of 20–200 mV/s (inset). The result suggests that the oxidation of three nitrophenol isomers at the nano-Au/GCE is a diffusion-controlled process.

3.6 Interferences

The interferences from some metal ions and other organic compounds were examined with 1×10^{-4} mol L^{-1} of nitrophenol isomers. The results indicated that they have no influence on the oxidation/reduction peak potential of the nitrophenol isomers. As a result, measurement of the peak height for three times and the average current values were obtained. If the presence of some metal ions and organic compound altered the current signal of nitrophenol isomers by less than ±5%, we consider that cause no interference. Some possible inorganic and organic compounds in the wastewater such as K^+, Mg^{2+}, NO_3^-, SO_4^{2-}, Ac^-, Cl^- (each of 1.0×10^{-2} mol L^{-1}) and 4-aminophenol, phenol, 4-chlorophenol, naphtalinum (each of 1.0×10^{-4} mol L^{-1}) were added. The results indicated that they have no influence on the signals of the nitrophenol isomers.

3.7 Reproducibility and stability of the nano-Au/GCE electrode

When new nano-Au/GCE electrode was kept in the absolute ethanol for a week at room temperature, the sensitivity remained more than 95% of the initial signal. In order to verify the reproducibility of the modified electrode, repetitive measurements were done for nitrophenol isomers mixture (each of 1.0×10^{-4} mol L^{-1}). The relative standard deviations (RSD) of peak height for nitrophenol isomers in five times were no more than 1.7% (*m*-), 2.4% (*p*-), and 2.1% (*o*-nitrophenol), separately. When the electrodes lost 10% of the initial signals, they were considered to clear the surface of the electrode. The way is that electrode scans from −0.6 to 0.6 V for 20 cycles in the ethanol in order to recover sensitivity of determination.

3.8 Calibration graphs and application to artificial wastewater samples

Under the optimum conditions, the linear relationships between the peak height and the concentration are obtained in the range of 1.0×10^{-5}–1.0×10^{-3} mol L^{-1} for *o*-nitrophenol; 7.5×10^{-6}–2.0×10^{-3} mol L^{-1} for *m*-nitrophenol; 1.0×10^{-5}–1.0×10^{-3} mol L^{-1} for *p*-nitrophenol, respectively. The limit of detection (LOD) is 8.0×10^{-6} mol L^{-1} for *o*-nitrophenol, 5.0×10^{-6} mol L^{-1} for *m*-nitrophenol and 8.0×10^{-6} mol L^{-1} for *p*-nitrophenol (at $S/N = 3$). Figure 7 shows the semi-derivative voltammograms and calibration graphs (Fig. 7 inset) of the solutions containing *o*-, *m*-, and *p*-nitrophenol.

We studied the applicability of the nano-Au/GCE by measuring local wastewater and tap water samples. The quantitative determination was performed by standard-addition method. The results are summarized in Table 1. The recovery of the samples ranged between 95.6 and 107%, verifying the possibility of the method.

4 Conclusions

The modified electrode (nano-Au/GCE) described in this article is very fast and easy to prepare, and it can absolutely separate three nitrophenol isomers and remarkably enhance the redox peak currents of nitrophenol isomers. Based on this, a very sensitive electrochemical method has been

Table 1 Determination of nitrophenol isomers in real samples

	Wastewater			Tap water		
	o-Nitrophenol	*m*-Nitrophenol	*p*-Nitrophenol	*o*-Nitrophenol	*m*-Nitrophenol	*p*-Nitrophenol
Content (10^{-5} mol L^{-1})	–	7.5	18	–	–	–
Added (10^{-5} mol L^{-1})	50	7.5	18	50	10	20
Found (10^{-5} mol L^{-1})	49.3	15.3	35.2	47.8	10.7	19.4
RSD (%, $n = 6$)	3.7	3.9	4.3	3.8	4.6	4.7
Recovery (%)	98.6	102	97.7	95.6	107	97

developed for the simultaneous determination of *o*-, *m*-, and *p*-nitrophenol.

Acknowledgments This project was supported by the National Natural Science Foundation of China (Grant No. 20975061), the National Basic Research Program of China (Grant No. 2007CB 936602), the Natural Science Foundation of Shandong Province in China (Grant No. Y2008B20).

Appendix

See Fig. 8.

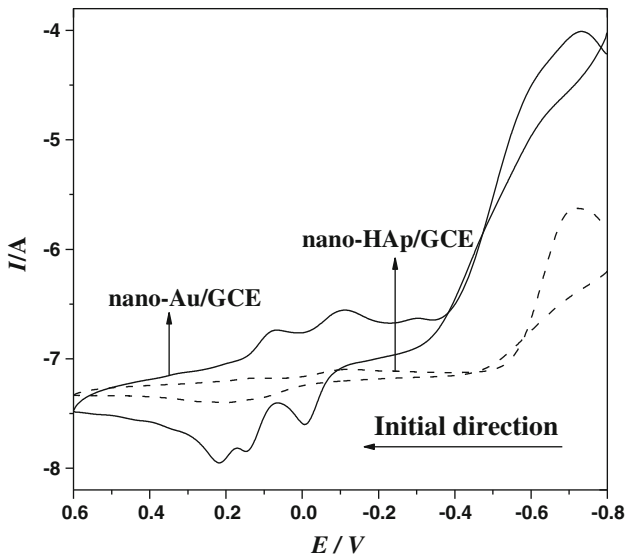

Fig. 8 The contrast response of the *o*-, *m*-, *p*-nitrophenol mixture (1×10^{-4} mol L^{-1} for each) in 0.1 mol L^{-1} Na_2HPO_4–NaH_2PO_4 (pH 6.0) buffer solution at nano-Au/GCE (*solid line*) and nano-HAp/GCE (*dash line*)

References

1. US Environmental Protection Agency (1989) Fed Regist 52:131
2. Niazi A, Yazdanipour A (2007) J Hazard Mater 146:421
3. Shkumbatiuk R, Bazel YR, Andruch V et al (2005) Anal Bioanal Chem 382:1431
4. Bravo R, Caltabiano LM, Barr DB et al (2005) J Chromatogr B 820:229
5. Yamauchi Y, Ido M, Maeda H et al (2004) Chem Pharm Bull 52:552
6. Ni YN, Wang L, Kokot S (2001) Anal Chim Acta 431:101
7. Hu SS, Xu CL, Wang GP et al (2001) Talanta 54:115
8. Huang WS, Yang CH, Zhang SH (2003) Anal Bioanal Chem 375:703
9. Zhang H, Wang ZH, Zhou SP (2005) Sci China B 48:177
10. Dai X, Nekrassova O, Compton RG et al (2004) Anal Chem 76:5924
11. Li Y, Shi GQ (2005) J Phys Chem B 109:23787
12. Zhang X, Shi F, Yu X et al (2004) J Am Chem Soc 126:3064
13. Goyal RN, Gupta VK, Oyama M et al (2007) Talanta 72:976
14. Zhuo Y, Yuan R, Chai YQ et al (2006) Biomaterials 27:5420
15. Dai J, Guo L, Jiang Y et al (2005) J Nanosci Nanotechnol 5:474
16. Li CX, Deng KQ, Shen GL et al (2004) Anal Sci 20:1277
17. Lei CX, Hu SQ, Yu RQ et al (2004) Bioelectrochemistry 65:33
18. Han L, Zhang XL (2009) Electroanalysis 21:124
19. Luo LQ, Zou XL, Ding YP et al (2008) Sens Actuators B 135:61
20. El Mhammedi MA, Achak M, Chtaini A et al (2009) J Hazard Mater 163:323
21. Forryan CL, Lawrence NS, Compton RG et al (2004) J Electroanal Chem 561:53
22. Luz RDCS, Damos FS, Kubota LT et al (2004) Talanta 64:935